Available online at www.sciencedirect.com
SCIENCE DIRECT®
Journal of Photochemistry and Photobiology A: Chemistry 163 (2004) 323–329
Journal of Photochemistry and Photobiology A:Chemistry
www.elsevier.com/locate/jphotochem

Thin-film transmission IR spectroscopy as an in situ probe of the gas–solid interface in photocatalytic processes

Sho Kataoka[1], M. Isabel Tejedor-Tejedor, Juan M. Coronado[2], Marc A. Anderson*

Environmental Chemistry & Technology Program, University of Wisconsin-Madison, 660 N. Park St. Madison, WI 53706, USA

Received 26 July 2003; received in revised form 31 December 2003; accepted 6 January 2004

Abstract

A thin-film transmission infrared spectroscopy system was designed as an in situ probe for heterogeneous interfacial photocatalytic reactions. A photocatalyst, TiO_2, supported on a silicon wafer substrate was located in an airtight cell containing BaF_2 windows. This supported photocatalyst was simultaneously illuminated with both UV light and the infrared beam. The performance of the cell was tested using the photocatalytic decomposition of ethanol. The quality of the spectra for a porous TiO_2 film of approximately 0.5 microns of thickness proved to be good for detecting bands of reactant and product species (ethanol, ethoxide, acetaldehyde, and acetate). This transmission cell was coupled to a gas phase infrared cell for the simultaneous analysis of reactants and products of this photodegradation of ethanol which appear in the gas phase. The affinity of the surface of TiO_2 for water was investigated under air and argon environments in both the presence and the absence of UV illumination. In an air environment, UV illumination enhanced the adsorption of water on TiO_2. A similar enhanced adsorption occurred in the argon environment without UV illumination. During UV illumination, bands of peroxide (O_2^{2-}) species could be detected on the surface of TiO_2 under the conditions of a dry air flow. Both peroxide (O_2^{2-}) as well as superoxide (O_2^-) species could be detected after several hours in post-irradiated systems.

Keywords: Transmission IR; Photocatalysis; Ethanol; Interfacial water; Peroxides; Superoxides; TiO_2; Surface species

1. Introduction

Photocatalytic reactions using TiO_2 as the semiconductor catalyst have been widely investigated for the past couple of decades as a potential technique for decomposing trace contaminants in both air and water [1–5]. Due to the strong oxidative capacity of this process, contaminants generally end up as harmless products, e.g., carbon dioxide and water. When TiO_2 is illuminated with ultraviolet irradiation (UV, shorter than ca. 400 nm in wavelength), electrons in the valence band are excited to the conduction band, leaving positive holes remaining in the valence band. These electrons and holes near the surface are trapped by surface species (e.g., adsorbed oxygen molecules and hydroxyl groups), which subsequently form active species (e.g., O_2^-, $OH^\bullet$, O^-) [6–9]. These active species, coupled with direct charge injection mechanisms, are capable of performing oxidation and reduction reactions which result in the decomposition of contaminants.

The concern for improved efficiency and superior reaction rates has stimulated investigations concerning photocatalytic reaction pathways. Many analytical techniques have been employed to identify and quantify reactants and products in this photocatalytic process. While photocatalytic decomposition reactions have been extensively studied, recent concern has also been focused on influence of UV light on the hydrophilicity of TiO_2 [10–14]. This event has been plausibly elucidated by the photo-stimulated structural changes of the air–TiO_2 interface [14–16]. By studying the nature of surface in the absence and presence of band-gap irradiation, one might better understand wetting characteristics and also better elucidate the nature of photocatalytic reactions in general.

Fourier transform infrared spectroscopy (FTIR) has constituted a powerful tool in studies concerning the nature of surface complexes at solid–gas and solid–liquid interfaces and has also been employed for in situ surface studies [17–24]. In order to use IR techniques as in situ probes to study photocatalytic reactions occurring on semiconductor surfaces, UV and IR irradiation need to be supplied

* Corresponding author. Tel.: +1-608-262-2674; fax: +1-608-262-0454.
E-mail address: nanopor@facstaff.wisc.edu (M.A. Anderson).
[1] Present address: Dr. Cremer Group, Department of Chemistry, Texas A&M University, 3255 TAMU College Station, TX 77843, USA.
[2] Present address: Instituto de Catálisis y Petroleoquímica, CSIC Campus Cantoblanco, C/Marie Curie s/n., 28047 Madrid, Spain.

1010-6030/$ – see front matter © 2004 Elsevier B.V. All rights reserved.
doi:10.1016/j.jphotochem.2004.01.004

simultaneously to the semiconductor. As some examples of IR technique applied to probing photocatalytic reactions, the diffuse reflectance technique has been employed with powdered nano-porous TiO_2 in the presence of UV light [25,26]. This system was shown to have a good signal-to-noise ratio (SNR) for adsorbed organic species and is an important contribution in the in situ analysis of photocatalytic reactions. However, since the depth of optical penetration of the IR beam into a scattering nano-porous grain of catalyst is much greater than that of UV, diffuse reflectance IR spectra show chemical bonds of both the fraction which is illuminated with UV light as well as that corresponding to the dark fractions of the grain. Thin-film transmission methods have been used for in situ monitoring of surface chemistry [27–29] and have been applied to a few photochemical or photocatalytic reactions [30–32]. The study [32] performing the photo-oxidation of dimethyl methylphosphonate monitored with IR transmission method used TiO_2 powder fixed on tungsten grid. Our concern about the optical penetration of UV light on TiO_2 mentioned above still remains. Attenuated total reflection–infrared spectroscopy (ATR–IR) is another potential technique for the in situ analyses of photocatalytic reactions. In this technique, a thin-film of TiO_2 should be coated onto the internal reflecting element (IRE, e.g., CaF_2, BaF_2, Si). A single bounce ATR–IR accessory has been used for in situ studies in liquid phase photocatalysis [33]. In addition to ATR–IR techniques, there are a few publications concerning surface-enhanced infrared absorption (SEIRA) for in situ analyses of photocatalytic reactions [34,35].

In our laboratory, sol–gel derived TiO_2 thin-films coated on supports have been intensively used for studies on the photocatalytic decomposition of trace contaminants in air. For the purpose of understanding our systems better, this study is addressed to observing photocatalytic reactions occurring at the solid–gas interface using IR spectroscopy in a similar manner, i.e., TiO_2 thin-film coated system. Hence, we demonstrate IR transmission methods that utilize a porous TiO_2 thin-film supported on a silicon (Si) wafer as a simple and less expensive system with which to probe photocatalytic reactions. Due to its high transmittance in the IR range (4000–6500 cm^{-1}), Si is commonly used as an optical window and an IRE material for FTIR studies [36]. It is not hygroscopic and is chemically stable even at temperatures higher than 350 °C. This means that Si can survive the high temperatures employed during the sintering of TiO_2 in order to obtain the desired catalyst from sol–gel processing. In addition, Si wafers are inexpensive (widely used for computer hard disks). More importantly, the investigation could be performed under a closed environment, and the system connected to another IR spectrometer for simultaneously monitoring gas phase composition. The decomposition of ethanol has been well investigated and several reaction pathways of the reaction have been proposed [26]. During photo-activation of TiO_2 thin-films, we investigated adsorbed water and oxygenated species that are produced on the TiO_2 porous film under controlled humidity conditions.

2. Experimental section

A TiO_2 sol was prepared via a sol–gel processing procedure [3] and was sprayed on one side of a Si wafer (2 in. in diameter, Silicon Quest International, Santa Clara, CA). The supported catalyst was dried at 100 °C and subsequently calcined at 350 °C for 3 h. This TiO_2 sol was sprayed five more times onto the previous TiO_2 surface and the calcination process was also repeated after the final coat. Based on measurements with an ellipsometer (Model L2W16C.830, Gaertner Scientific Corp., Skokie, IL), the thickness of TiO_2 thin-film was shown to be 470 nm, and the refractive index was 1.72. Assuming dry conditions and that a single crystal TiO_2 has a refractive index of 2.52 (anatase), the porosity of the film is estimated to be 52.6%.

The thickness of the Si wafer, used as the support for the TiO_2 thin-films of interest, influences the quality of the spectra in more than one way. The transmission of IR radiation is higher in the case of thinner Si wafers, and SNR of the IR spectra becomes larger. However, from a preliminary experiment where a thin Si wafer (295 μm in thickness) was applied, interference fringes were superimposed upon the spectra of the sample, and intense fringes of the appropriate frequency may greatly decrease the quality of the IR spectra. Therefore, all subsequent results were obtained using Si wafers of 615 μm in thickness as a supporting material.

A schematic diagram and photograph of the in situ IR cell are shown in Fig. 1(a) and (b), respectively. The catalyst (TiO_2 supported on the Si wafer) was located in the gap between two borosilicate glass discs, which were separated by a viton o-ring and fastened with aluminum plates. For convenience, this entire assembly is hereafter referred to as "the cell." Each borosilicate glass disc has a hole (3/8 in. in diameter) in the center that is covered with a BaF_2 disc. This material is optically transparent between 10,000 and 700 cm^{-1} and serves as windows for the input and output of the IR irradiation in the cell (note that borosilicate glass is opaque below ca. 2000 cm^{-1}). In addition to the IR windows, each of the borosilicate discs contains an inserted piece of glass tubing (1/4 in. in diameter) that functions as inlet and outlets for the gas stream.

For collecting IR spectra, the cell was positioned perpendicularly to the direction of the IR beam in the sample chamber of an IR spectrophotometer (Nexus 670, Nicolet Instrument, Madison, WI). The spectrophotometer contained an MCT-A (HgCdTe) detector and KBr beam splitter. The aperture of the beam was chosen to be such that the IR was confined to enter only through the BaF_2 window. Recorded spectra were the result of 100 co-added interferograms with a resolution of 4 cm^{-1}. The spectral region of our investigations was between 4000 and 700 cm^{-1}. A light source for photocatalytic reactions (a 200-W medium pressure Hg

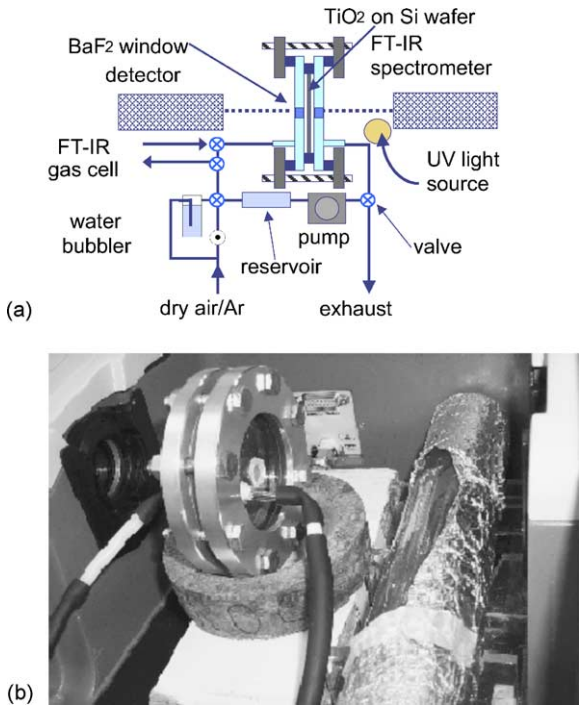

Fig. 1. (a) Schematic diagram of the system used for in situ probing of photocatalytic reactions using the thin-film transmission IR cell. (b) Picture taken of the thin-film transmission IR cell in the sample chamber of an IR spectrophotometer.

vapor lamp, Model 7825-32, Ace Glass, Vineland, NJ) covered with a cooling jacket of water was positioned in the chamber. The photocatalyst was fully illuminated with UV light from outside of the cell, and its intensity was measured to be ca. 6 mW/cm^2 at the position of the surface of the TiO_2 catalyst using a photo detector (International Light Inc., Newburyport, MA).

The photocatalytic decomposition of ethanol was conducted as a method of confirming the performance of the cell. The transmission cell was connected to a reservoir and a pump (Model QD, Fluid Metering Inc., Syosset, NY), forming a closed-cycle system (total volume of this system was 1.1 l). The closed-cycle system was also connected to an FTIR multiple reflection gas sampling cell (Model 4.8-PA, Infrared Analysis Inc., Anaheim, CA), which was located in another FTIR spectrometer (Magna 750 series II, Nicolet Instruments, Madison, WI) for determining the nature and concentration of compounds in the gas phase of the reactor. Initially, 17.2 μmol of liquid ethanol was injected into this system yielding a concentration of ethanol in gas phase of 15.7 μM (3.8×10^{-4} atm).

The effect of humidity on the surface of the TiO_2 catalyst was investigated in both the presence and absence of UV illumination. The experiments (20, 40, 60% relative humidity) were carried in a single pass mode using a stream of air or Ar, and by adjusting the relative humidity of the flow. All gases used in the experiments were directly dispensed from cylinders (zero air; RH < 0.2% and ultra-pure Ar). The humidity was measured both with a humidity probe (Model HM 34, Vaisala, Helsinki, Finland) and the FTIR gas cell detecting water vapor. The humidity was controlled by blending the dry flow with another stream that was humidified by passing through a water bubbler. After passing dry air over night (air or Ar without CO_2 and H_2O), a background spectrum was collected. In the last section of this paper, we also discuss the presence of oxygen species on TiO_2 films. The spectra were obtained in the same way as in the humidity study, and TiO_2 films were also observed after the UV irradiation.

3. Results and discussion

3.1. Photocatalytic decomposition of ethanol

IR spectral information on the photocatalytic oxidation of ethanol was collected using both the thin-film TiO_2 transmission cell for the surface species as well as the gas sampling cell for gaseous compounds. Although this study did not provide quantitative information concerning species on the surface of TiO_2, there is the opportunity to perform quantitative analysis for adsorbed organics by previously calibrating the transmission cell. If the calibration experiment is performed with a cell of known TiO_2 film thickness (the optical path length) the extinction coefficient of these adsorbed species can be calculated. The same can be true for the reaction products, although, in this case the cell calibration may be less direct.

Spectra in Fig. 2 were recorded with the Si wafer cell. The spectrum in Fig. 2(a) was obtained at equilibrium after providing ethanol to the system before illuminating with UV light. The bands observed at 1266, 1093, 1051 and 885 cm^{-1} are due to molecularly adsorbed ethanol and those at 1420, 1378, 1131 and 1072 cm^{-1} are associated with ethoxide vibrations [26,37,38]. The peak at 1051 cm^{-1} has also been attributed to a bridging ethoxy complexes [37,38], however the presence of free ethanol in the spectrum does not allow one to definitively describe the formation of this bridging complex. The band which appears as a negative band at

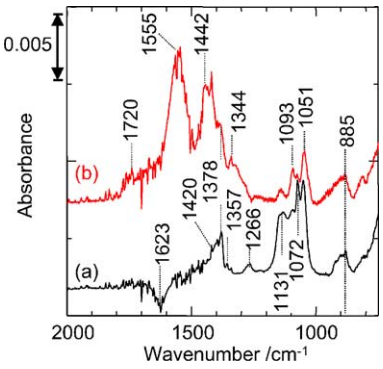

Fig. 2. Thin-film transmission spectra of the photocatalytic decomposition of ethanol: (a) before UV illumination, (b) after 3 h of UV illumination.

Table 1
Assignment of the FTIR bands observed in the photocatalytic decomposition of ethanol on TiO_2

Species	Vibration mode	Frequency (cm^{-1})	
		Experiment	Literature
Ethanol	δ(OH)	1266	1264
	ν(C–C)	1093	1093
	ν(C–O)/C–C	1051	1042
	ρ(C–H)	885	
Ethoxide	$\delta(CH_2)$ scissoring	–	1473
	$\delta(CH_3)$	1420	1447
	$\delta(CH_3)$	1378	1379
	CH_2 wagging	1357	1356
	ν(C–O) monodentate	1131	1144
	ν(C–O) monodentate		1119
Acetate	ν_{as}(COO) bridging	1555	1535
	ν_s(COO) bridging	1442	1453
Acetaldehyde	ν(C=O)	1740	1715/1718

Literature [26,37,38].

the frequency of the bending mode of adsorbed water, 1623 cm^{-1}, can be attributed to the desorption of water caused by the formation of the ethoxide species. Fig. 2(b) belongs to the adsorption spectrum taken three hours after starting UV illumination. This spectral feature is different from the spectrum recorded before UV illumination, and the major adsorption bands that now appear at 1555 and 1442 cm^{-1}, can be assigned to the by-product acetate ions that form a bridging bidentate complex with the TiO_2 surface [37,38]. The presence of bands at 1378, 1093, 1079, 1046, and 885 cm^{-1} suggests that the reactants, mainly ethanol, still remain on the surface of TiO_2. We attribute the weak and unresolved broad band in the region 1740–1620 cm^{-1} to the absorption by carbonyl groups of molecularly adsorbed acetaldehyde molecules and monodentate acetates. Acetaldehyde is an expected by-product of photodegrading ethanol. The band near 1344 cm^{-1} can be due to the ν_{C-O} mode of the monodentate acetate. Table 1 presents a summary of all bands in the above mentioned spectra and also a more detailed band assignment.

Fig. 3 shows the gas phase IR spectra of the system taken with the second IR spectrophotometer that contains the gas sampling system that is placed in series with the transmission IR cell. Fig. 3(a) was obtained at the same instant as Fig. 2(a), and likewise Fig. 3(b) was taken at the same moment as that of Fig. 2(b). Gas-phase ethanol bands at 3677, 2974, 2904, 1394, 1242, 1064, and 877 cm^{-1} decreased during the course of the 3 h UV illumination. Subsequently, bands attributed to oxidation reaction products such as acetaldehyde at 2710 and 1766 cm^{-1} and carbon dioxide at 2365 cm^{-1} started to appear. By coupling these two tandem IR techniques in series, we can simultaneously follow the reaction on the surface as well as identify products and reacting species in the gas phase.

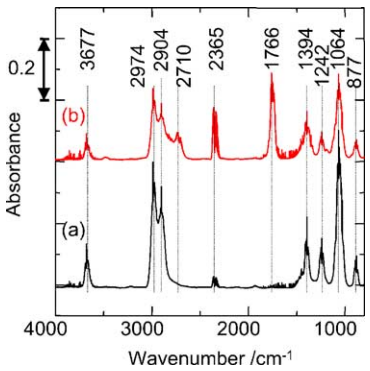

Fig. 3. Gas-phase IR spectra of the photocatalytic decomposition of ethanol: (a) before UV illumination, (b) after 3 h of UV illumination.

3.2. Photo-enhanced water adsorption

This section concerns the affinity of TiO_2 for water under different conditions and searches for clues to better understand the photo-enhanced wetting ability of TiO_2. Spectra in Fig. 4(a–d) belong to the same TiO_2 film exposed to oxic and anoxic environments (air and Ar), three different conditions of humidity (20, 40, and 60% RH at 23 °C) and correspond to experiments conducted in both the presence and absence of UV illumination. These experiments were performed in a single pass gas stream, and the outlet gas was monitored with a temperature and humidity probe. The temperature of the sample did not increase during the course of the experiments. It should also be noted that some spectra contained many sharp peaks (between 4000 and 3600 cm^{-1}) due to water molecules in gas phase. Considering the short optical path length of the transmission cell, these peaks are mostly caused by water molecules outside of the cell and have been ignored in the present study.

In this study, the tendency for the TiO_2 porous film to retain interfacial water and/or OH under different environments will be measured by the intensity of the bands,

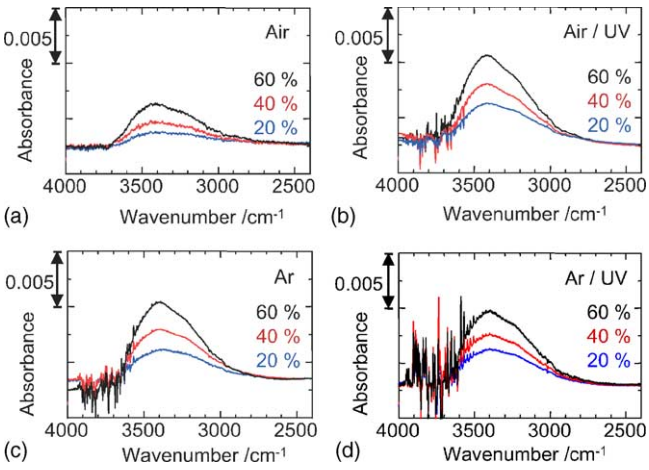

Fig. 4. Spectra showing O–H stretching bands under different conditions of humidity for the comparison of water adsorption under the condition of: (a) in air without UV illumination, (b) in air with illumination, (c) in Ar without illumination, (d) in Ar with illumination.

associated with the $\nu_{(O–H)}$ vibration modes, that appear in the region of 3700–2800 cm^{-1}. Fig. 4 exemplifies this spectral region of 4000–2400 cm^{-1} for the different conditions studied. All spectra in this figure are plotted on the same scale. Each section of this figure (a–d) contains the spectra of the TiO_2 film under three different humidity conditions (from bottom to top: 20, 40, and 60% RH) while keeping unchanged the remaining tested variables. A comparative examination of Fig. 4(a) and (b) reveals that the intensity of bands in the presence of UV illumination approximately doubles over that in its absence, which indicates that UV illumination increased the affinity of TiO_2 for adsorbing water. These results correspond to the published reports concerning the photo-enhanced wetting ability of water [15–20]. We can now see quite directly the photo-enhanced adsorption of water using this IR technique. A few recent publications [12,20] that have reported on the photo-enhanced wetting ability of TiO_2 using FTIR claimed the appearance of a new O–H stretching peak upon UV illumination at 3695 cm^{-1} or 3716 cm^{-1}. Another publication maintained that the maximum in the spectral absorption band of adsorbed water was shifted to lower frequency (from 3500 to 3450 cm^{-1}) upon UV illumination [34]. However, it should be noted that we observed neither of these events in this present study. It may be because of the short of IR path length of TiO_2 and/or the shifts in frequency due to using Si wafer support [39], and in order to minimize these difficulties, the system needs to be improved such as by providing narrow band-pass filters [28].

The TiO_2 surface in a dark Ar environment (Fig. 4(c)) adsorbed a larger quantity of water than that in air (Fig. 4(a)) and almost the same quantity as that illuminated with UV light in air (Fig. 4(b)). In the Ar environment, additional adsorption of water upon illumination by UV light was minimal. (Compare Figs. 4(c) and (d)) Previous reports examined the desorption behavior of oxygen on TiO_2 under UV illumination [40,41]. Furthermore, some research has suggested that water strongly adsorbs on the oxygen defects [8,13,14]. In the current study, the surface in an anoxic environment (Ar) had similar O–H features of IR bands to that same TiO_2 surface in the air under UV illumination. The results lead us to believe that oxygen, which adsorbs on the TiO_2 surface prior to supplying water, partially hinders water adsorption.

3.3. Oxygen species

In this section, we investigate the formation of reduced oxygen species on the TiO_2 (i.e., peroxides and superoxides) upon UV irradiation in air, and their subsequent evolution after the irradiation. Due to the fact that molecular oxygen is a good electron scavenger, peroxide and superoxide complexes are expected to form on the surface of UV-activated TiO_2. In principle, since their $\nu_{(O–O)}$ stretching mode is active in IR, it should be possible to identify these species by vibrational spectroscopy in principle. In order to distinguish features caused by the separation of holes and electrons in the UV-activated TiO_2 spectrum from those due to reduced oxygen, we performed experiments in both air and Ar atmospheres.

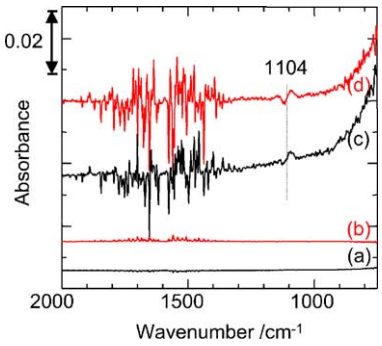

Fig. 5. Spectra with interference by UV illumination under the condition of: (a) in air without UV illumination, (b) in Ar without illumination, (c) in air with illumination, (d) in Ar with illumination.

Reported frequency values for the $\nu_{(O–O)}$ stretching mode of metal superoxide complexes range between 1145 and 1096 cm^{-1} [42]. Corresponding to their lower O–O bond order, metal peroxide complexes absorb at considerable lower frequencies than superoxides. Frequency for the $\nu_{(O–O)}$ mode in peroxide species is in the range from 770 cm^{-1} (in the case of H_2O_2) to even higher than 900 cm^{-1} for some bridging peroxides [43–45]. The frequency of the $\nu_{(O–O)}$ of metal-peroxo species is in inverse relation to the magnitude of charge transfer from the ligand to the metal [44]. The frequency of this vibration also depends on the density of the peroxo ligand in relation to the metal (side-on versus end-on types) [42,44,45]. Diperoxo (side-on) complexes absorb at lower energies than monoperoxo complexes (end-on). Also, the protonation of a end-on complex reduces the frequency of the $\nu_{(O–O)}$ vibration.

Fig. 5(a) and (b) represent the 100% line (calculated by taking the ratio of two sample spectra under identical conditions) of the transmission cell with the TiO_2 film before UV illumination, under 0% RH, in air and in Ar environments respectively. These 100% lines illustrate the SNR of the spectra obtained under these experimental conditions. Spectra in Fig. 5(c) and (d) represent the spectrum of UV-illuminated TiO_2 in air and in Ar atmospheres respectively, using as a background the spectrum collected before UV illumination. The spectra of Fig. 5(c) and (d) show an increase in absorption below 850 cm^{-1}. Unfortunately, the exact position of this band is unknown since its absorption maximum is below the cut-off of this system. The intensity of the band in the spectrum recorded in air is larger than in the spectrum recorded in Ar. This is particularly obvious in the range between 900 and 850 cm^{-1}. In addition, the first derivative peaks centered at 1104 cm^{-1} are only significant under UV illumination. The background spectrum of a Si wafer coated with TiO_2 (not shown) has a sharp edge centered at 1104 cm^{-1}, which is in the exact same position as the first derivative peaks. Hence, those peaks were

presumably caused by the interference of the sharp edge due to UV illumination.

Since Ar is an inert gas in IR, any features of the spectrum in Ar, Fig. 5(d) (except for water vapor bands associated with fluctuations in humidity of the atmosphere outside of the transmission cell) should be attributed to differences in the structure of the TiO_2 introduced by activation with UV light. Separation of holes and electrons upon illumination should generate changes in the bond order of Ti–O groups (Ti^{3+}–O^-). It has been reported that the presence of oxygen vacancies produces significant broadening and high-frequency shifts of the main anatase band [42] (the major absorption band for non-activated TiO_2 is expected to appear below 800 cm^{-1}). As mentioned above that metal peroxo complexes absorb between 900 and 750 cm^{-1}, the formation of peroxo complexes on the surface of the activated TiO_2 in the presence of air should account for the larger intensity of absorption below 850 cm^{-1} in spectrum of Fig. 5(c) than in the spectrum of Fig. 5(d).

Spectra in Fig. 6 were recorded in a dry air environment after stopping UV illumination. The intense absorption band (around 800 cm^{-1}) present in the spectra of Fig. 6 (0 h) decreases rapidly after terminating UV irradiation and new bands, 1138, 1028, and 836 cm^{-1}, start growing-in as a function of time and are still present in the spectrum after 10 h of flowing dry air past the sample. These bands were not observed in an Ar environment. When water was supplied, these bands disappeared very quickly. It has been previously reported that superoxides and peroxides are formed on the surface of TiO_2 after being illuminated with UV light [7,46,47]. Furthermore, as stated above, frequency values for the $\nu_{(O–O)}$ mode of metal superoxides complexes range between 1145 and 1097 cm^{-1} and metal peroxides between 900 and 750 cm^{-1} [37,42–45]. Supporting these findings, our IR studies here confirm that, in the presence of air, UV illumination of the TiO_2 generates surface peroxide complexes (absorption below 850 cm^{-1}). However, no superoxide species (absorption bands between 1145 and 1097 cm^{-1}) are appreciable in spectrum of Fig. 5(c) during illumination. After stopping illumination, a fraction of the peroxides

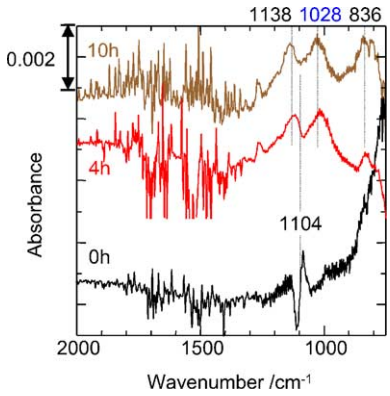

Fig. 6. Spectra showing oxygenated species upon finishing the UV illumination after 0, 4, and 10 h of irradiation.

species will react with more O_2 molecules to form surface superoxides (O_2^{2-} (ads) + O_2 (g) → $2O_2^-$ (ads)), and new absorption bands associated with these species appear in the spectrum, Fig. 6 (10 h). Although the lifetime of the peroxides (O_2^{2-}) is significantly smaller in water (ca. 50 μs) [8,9], some recent publications [48–50] have claimed that the lifetime of electrons and holes are considerably extended under dry conditions or under a vacuum.

4. Conclusion

In this paper we have demonstrated the feasibility of obtaining good quality IR transmission spectra of surface species of UV-illuminated porous TiO_2 films, having a thickness in the range of 0.5 μ. By increasing the thickness of the TiO_2 film to 1 μ (e.g., TiO_2 films coated on both sides of TiO_2), the SNR of this particular cell configuration would increase without decreasing the effectiveness of UV illumination. The thickness of Si supports influences the quality of the spectra. Thicker Si wafers (i.e., 615 μ), in spite of being less IR transparent, avoid the problem of producing interference fringes that would appear as undesired spectral features.

The use of this transmission cell has provided the opportunity to investigate photocatalytic reactions in an in situ fashion. The integration of this cell in series with an in situ analytical tool for the gas phase (as for example the gas IR cell used in these studies) is feasible and provides simultaneous data from the two phases of the catalytic system. Before illumination, the species on the surface of the TiO_2 are molecularly adsorbed ethanol and ethoxy complexes. Also, the adsorption of ethanol provokes the displacement of some water molecules. After illumination, a bridging bidentate acetate complex forms as a major by-product on the surface of the TiO_2.

By using the transmission cell, the photo-enhanced adsorption of water on the illuminated catalyst surface has been confirmed. A similar enhanced adsorption of water was realized under an Ar environment without UV illumination. This fact may suggest that oxygen in air interferes with the adsorption of water and that UV illumination facilitates the oxygen desorption.

As stated above, we have observed the formation of peroxides on the surface of TiO_2 during the illumination and superoxides in post-illuminated condition. These findings show that UV illumination of TiO_2 thin-films produces, in addition to the rapid processes associated with the charge separation, long term modification of the surface of these materials.

Acknowledgements

The authors acknowledge Cardinal CG Inc. (Spring Green, WI) for the financial support. We also thank

Mr. Jeffrey R.S. Brownson for assisting the catalysts preparation.

References

[1] M.R. Hoffmann, S.T. Martin, W.Y. Choi, D.W. Bahnemann, Chem. Rev. 95 (1995) 69.
[2] J. Peral, X. Domenech, D.F. Ollis, J. Chem. Technol. Biotechnol. 70 (1997) 117.
[3] X.Z. Fu, L.A. Clark, W.A. Zeltner, M.A. Anderson, J. Photochem. Photobiol. A: Chem. 97 (1996) 181.
[4] M.E. Zorn, D.T. Tompkins, W.A. Zeltner, M.A. Anderson, Appl. Catal. B: Environ. 23 (1999) 1.
[5] S. Kataoka, D.T. Tompkins, W.A. Zeltner, M.A. Anderson, J. Photochem. Photobiol. A: Chem. 148 (2002) 323.
[6] D.W. Bahnemann, M. Hilgendorff, R. Memming, J. Phys. Chem. B 101 (1997) 4265.
[7] J.M. Coronado, A.J. Maira, J.C. Conesa, K.L. Yeung, V. Augugliaro, J. Soria, Langmuir 17 (2001) 5368.
[8] K. Ishibashi, A. Fujishima, T. Watanabe, K. Hashimoto, J. Phys. Chem. B 104 (2000) 4934.
[9] K. Ishibashi, Y. Nosaka, K. Hashimoto, A. Fujishima, J. Phys. Chem. B 102 (1998) 2117.
[10] R. Wang, K. Hashimoto, A. Fujishima, M. Chikuni, E. Kojima, A. Kitamura, M. Shimohigoshi, T. Watanabe, Nature 388 (1997) 431.
[11] R. Wang, K. Hashimoto, A. Fujishima, M. Chikuni, E. Kojima, A. Kitamura, M. Shimohigoshi, T. Watanabe, Adv. Mater. 10 (1998) 135.
[12] R. Wang, N. Sakai, A. Fujishima, T. Watanabe, K. Hashimoto, J. Phys. Chem. B 103 (1999) 2188.
[13] T. Watanabe, A. Nakajima, R. Wang, M. Minabe, S. Koizumi, A. Fujishima, K. Hashimoto, Thin Solid Films 351 (1999) 260.
[14] R.D. Sun, A. Nakajima, A. Fujishima, T. Watanabe, K. Hashimoto, J. Phys. Chem. B 105 (2001) 1984.
[15] M.A. Henderson, Langmuir 12 (1996) 5093.
[16] M.A. Henderson, Surf. Sci. Rep. 46 (2002) 5.
[17] A.J. Maira, J.M. Coronado, V. Augugliaro, K.L. Yeung, J.C. Conesa, J. Soria, J. Catal. 202 (2001) 413.
[18] L.D. Tickanen, M.I. Tejedor-Tejedor, M.A. Anderson, Langmuir 13 (1997) 4829.
[19] P.A. Connor, K.D. Dobson, A.J. McQuillan, Langmuir 11 (1995) 4193.
[20] S. Sakohara, L.D. Tickanen, M.A. Anderson, J. Phys. Chem. 96 (1992) 11086.
[21] M.R. Dhananjeyan, E. Mielczarski, K.R. Thampi, P. Buffat, M. Bensimon, A. Kulik, J. Mielczarski, J. Kiwi, J. Phys. Chem. B 105 (2001) 12046.
[22] A.L. Goodman, E.T. Bernard, V.H. Grassian, J. Phys. Chem. A 105 (2001) 6443.
[23] P.J. Thistlethwaite, M.S. Hook, Langmuir 16 (2000) 4993.
[24] K.D. Dobson, A.J. McQuillan, Phys. Chem. Chem. Phys. 2 (2000) 5180.
[25] S.H. Szczepankiewicz, A.J. Colussi, M.R. Hoffmann, J. Phys. Chem. B 104 (2000) 9842.
[26] J.M. Coronado, S. Kataoka, M.I. Tejedor-Tejedor, M.A. Anderson, J. Catal. 219 (2003) 219.
[27] C.N. Rusu, J.T. Yates, J. Phys. Chem. B 104 (2000) 12292.
[28] C.P. Tripp, M.L. Hair, Appl. Spectrosc. 46 (1992) 100.
[29] A.Y. Fadeev, R. Helmy, S. Marcinko, Langmuir 18 (2002) 7521.
[30] E.A. Wovchko, J.T. Yates, J. Am. Chem. Soc. 120 (1998) 10523.
[31] E.A. Wovchko, J.T. Yates, J. Am. Chem. Soc. 120 (1998) 7544.
[32] C.N. Rusu, J.T. Yates, J. Phys. Chem. B 104 (2000) 12299.
[33] G.N. Ekstrom, A.J. McQuillan, J. Phys. Chem. B 103 (1999) 10562.
[34] R. Nakamura, K. Ueda, S. Sato, Langmuir 17 (2001) 2298.
[35] R. Nakamura, S. Sato, Langmuir 18 (2002) 4433.
[36] S.K. Coulter, M.P. Schwartz, R.J. Hamers, J. Phys. Chem. B 105 (2001) 3079.
[37] K. Nakamoto, Infrared and Raman Spectra of Inorganic and Coordination Compounds, fifth ed., Wiley, New York, 1997.
[38] W.C. Wu, C.C. Chuang, J.L. Lin, J. Phys. Chem. B 104 (2000) 8719.
[39] J.K. Cox, C.P. Tripp, Appl. Spectrosc. 54 (2000) 144.
[40] C.N. Rusu, J.T. Yates, Langmuir 13 (1997) 4311.
[41] C.L. Perkins, M.A. Henderson, J. Phys. Chem. B 105 (2001) 3856.
[42] J.C. Parker, R.W. Siegel, J. Mater. Res. 5 (1990) 1246.
[43] C. Li, K. Domen, K. Maruya, T. Onishi, J. Chem. Soc., Chem. Commun. (1988) 1541.
[44] M.S. Reynolds, A. Butler, Inorg. Chem. 35 (1996) 2378.
[45] M. Selke, M.F. Sisemore, R.Y.N. Ho, D.L. Wertz, J.S. Valentine, J. Mol. Catal. A: Chem. 117 (1997) 71.
[46] Y. Nosaka, Y. Yamashita, H. Fukuyama, J. Phys. Chem. B 101 (1997) 5822.
[47] T. Hirakawa, Y. Nakaoka, J. Nishino, Y. Nosaka, J. Phys. Chem. B 103 (1999) 4399.
[48] C.J.G. Cornu, A.J. Colussi, M.R. Hoffmann, J. Phys. Chem. B 105 (2001) 1351.
[49] S.H. Szczepankiewicz, J.A. Moss, M.R. Hoffmann, J. Phys. Chem. B 106 (2002) 7654.
[50] S.H. Szczepankiewicz, J.A. Moss, M.R. Hoffmann, J. Phys. Chem. B 106 (2002) 2922.